Structural and computational insights into the SARS-CoV-2 Omicron RBD-ACE2 interaction

Jun Lan[1,*], Xinheng He[2,*], Yifei Ren[1,6,*], Ziyi Wang[1,*], Huan Zhou[3], Shilong Fan[1], Chenyou Zhu[4], Dongsheng Liu[4], Bin Shao[2], Tie-Yan Liu[2], Qisheng Wang[3], Linqi Zhang[5,#], Jiwan Ge[1,6,#], Tong Wang[2,#], Xinquan Wang[1,#]

[1]The Ministry of Education Key Laboratory of Protein Science, Beijing Advanced Innovation Center for Structural Biology, Beijing Frontier Research Center for Biological Structure, Collaborative Innovation Center for Biotherapy, School of Life Sciences, Tsinghua University, 100084 Beijing, China

[2]Microsoft Research Asia, Beijing, China.

[3]Shanghai Synchrotron Radiation Facility, Shanghai Advanced Research Institute, Chinese Academy of Sciences, Shanghai 201204, China

[4]Department of Chemistry, Tsinghua University, 100084 Beijing, China

[5]Center for Global Health and Infectious Diseases, Comprehensive AIDS Research Center, and Beijing Advanced Innovation Center for Structural Biology, School of Medicine, Tsinghua University, Beijing 100084, China

[6]Tsinghua-Peking Center for Life Sciences, Beijing, China

*These authors contributed equally to this work.

[#]Correspondence: zhanglinqi@mail.tsinghua.edu.cn, (L.Z.), gejw@mail.tsinghua.edu.cn (J. G.), watong@microsoft.com (T.W.), xinquanwang@mail.tsinghua.edu.cn (X.W.)

Extended Data Table 1 | Data collection and refinement statistics

	Omicron RBD - ACE2
Data collection	
Space group	$P4_12_12$
Cell dimensions	
a, b, c (Å)	104.71, 104.71, 227.10
α, β, γ (°)	90, 90, 90
Resolution (Å)	50-2.60(2.66-2.60)
R_{merge}	0.26 (2.45)
I/sI	11.3 (1.3)
Completeness (%)	99.77(98.58)
Redundancy	14.1 (11.2)
Refinement	
Resolution (Å)	36.54-2.60
No. reflections	39525
R_{work}/R_{free}	19.2/23.1
No. atoms	
Protein	6440
Ligand/ion	96
Water	131
B-factors	
Protein	50.47
Ligand/ion	90.06
Water	45.36
R.m.s. deviations	
Bond lengths(Å)	0.008
Bond angles (°)	0.93
Ramachandran	
Favored (%)	96.95
Allowed (%)	3.05
Outliers (%)	0.00

Extended Data Table 2 | Contact residues of the WT and Omicron RBD-ACE2 interfaces

ACE2	WT RBD	Omicron RBD
S19		A475, N477
Q24	A475, N487	A475, N477, N487
T27	F456, A475, Y489	F456, Y489
F28	Y489	Y489
D30	K417, F456	
K31	Y489, Q493	F456, Y489
H34	Y453, L455, Q493	Y453, K493, S494
E35	Q493	K493
E37	Y505	
D38	Y449	Y449, S496, R498
Y41	Q498, T500, N501	R498, T500, Y501
Q42	G446, Y449, Q498	Y449, R498
L79	F486	F486
M82	F486	F486
Y83	F486, N487, Y489	F486, N487, Y489
N330	T500	T500
K353	G496, N501, G502, Y505	Y501, G502, H505
G354	G502	G502, H505
D355	T500	T500
R357	T500	T500
R393	Y505	

A distance cut-off of 4 Å was used.

Extended Data Table 3 | The hydrogen bonds and salt bridges at the WT and Omicron RBD-ACE2 interfaces

	WT RBD	Length(Å)	ACE2	Length(Å)	Omicron RBD
Hydrogen bonds			S19(O)	3.2	N477(ND2)
			S19(OG)	3.1	A475(O)
			S19(N)	3.4	N477(OD1)
	N487(ND2)	2.6	Q24(OE1)	2.8	N487(ND2)
	K417(NZ)	3.0	D30(OD2)		
			H34(ND1)	2.9	Y453(OH)
	Q493(NE2)	2.8	E35(OE2)	3.1	K493(NZ)
	Y505(OH)	3.2	E37(OE2)		
			D38(OD1)	2.9	R498(NH1)
			D38(OD1)	2.8	S496(OG)
	Y449(OH)	2.7	D38(OD2)	2.5	Y449(OH)
	T500(OG1)	2.6	Y41(OH)	2.6	T500(OG1)
	N501(N)	3.7	Y41(OH)		
	G446(O)	3.3	Q42(NE2)		
	Y449(OH)	3.0	Q42(NE2)	3.4	Y449(OH)
	Y489(OH)	3.5	Y83(OH)	3.5	Y489(OH)
	N487(OD1)	2.7	Y83(OH)	2.4	N487(OD1)
	G502(N)	2.8	K353(O)	2.7	G502(N)
	Y505(OH)	3.7	R393(NH2)		
Salt bridges	K417(NZ)	3.9	D30(OD1)		
	K417(NZ)	3.0	D30(OD2)		
			E35(OE2)	3.1	K493(NZ)
			D38(OD1)	2.9	R498(NH1)
			D38(OD1)	3.7	R498(NH2)

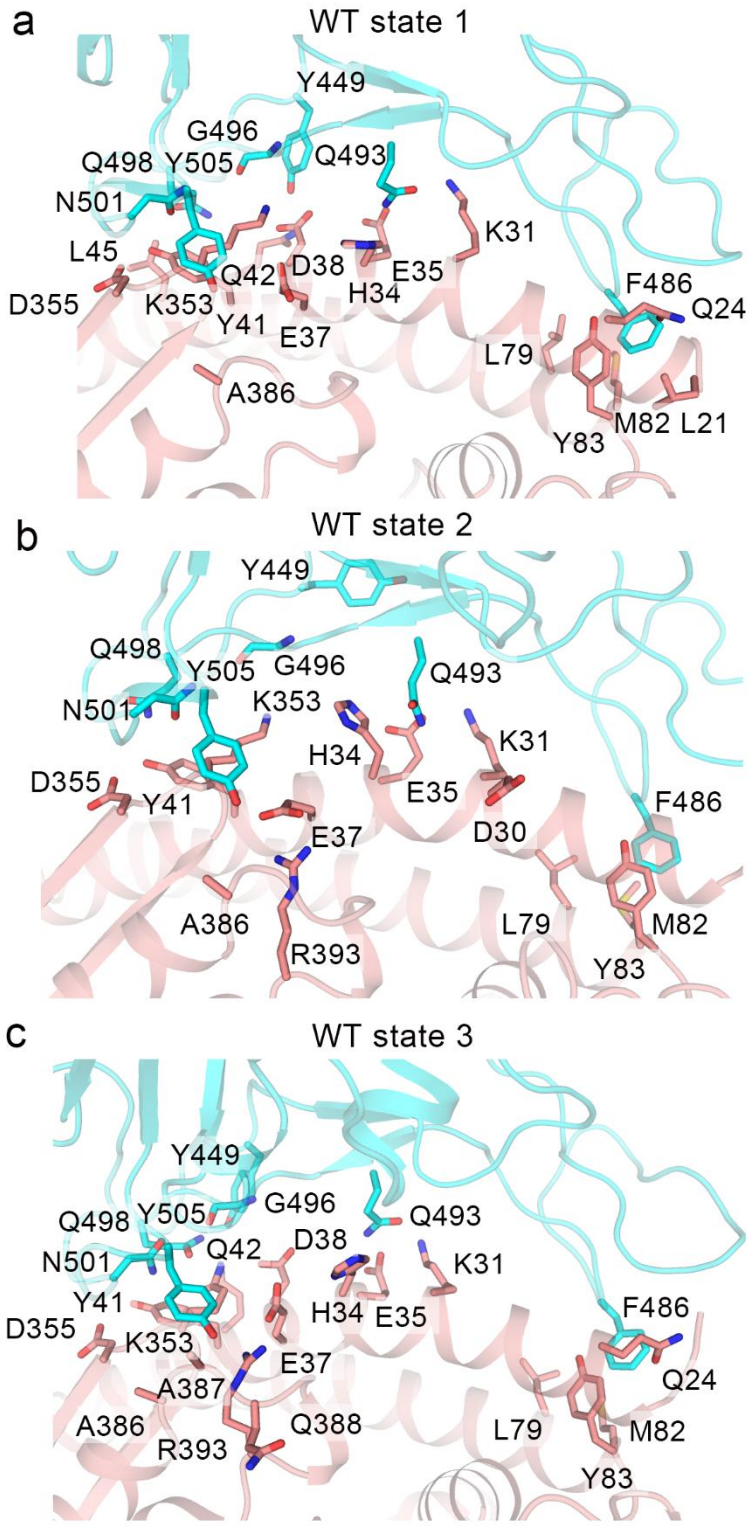

Extended Data Fig. 1 The interactions between ACE2 and RBD in different WT states. The residues in ACE2 within 5 Å to Y449, F486, Q493, G496, Q498, N501, and Y505 are shown in sticks. The RBD of WT and ACE2 are shown in cyan and salmon, respectively.

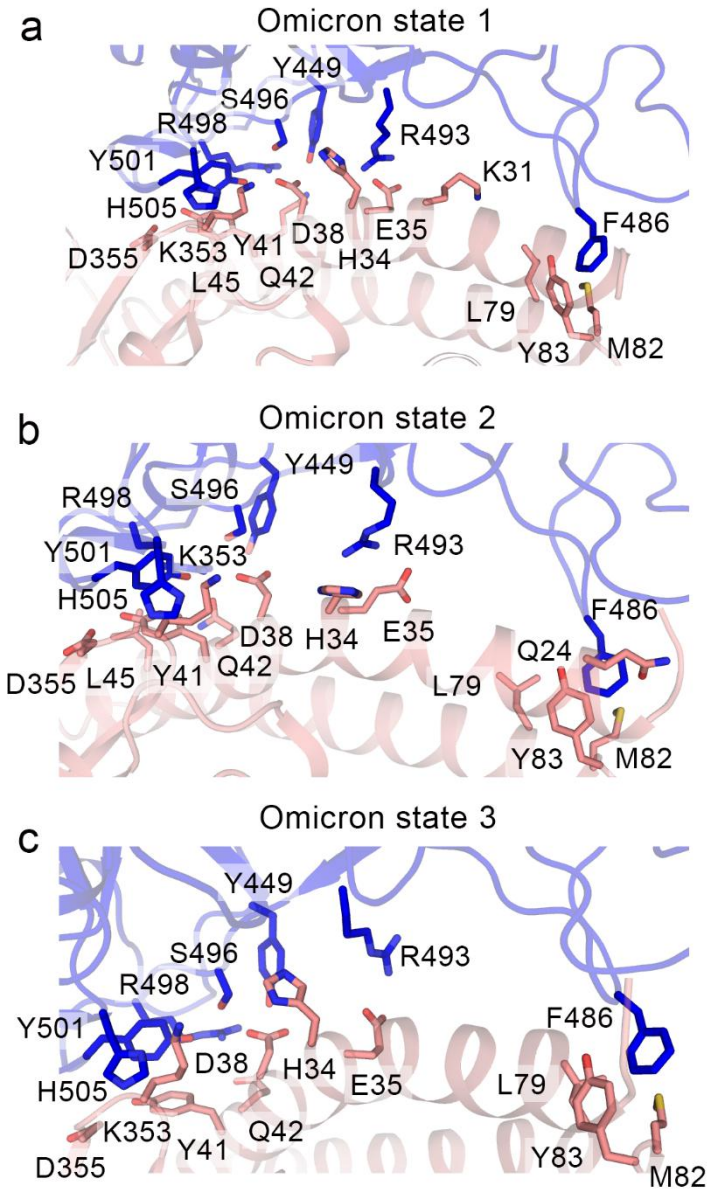

Extended Data Fig. 2 The interactions between ACE2 and RBD in different Omicron states. The residues in ACE2 within 5 Å to Y449, F486, R493, S496, R498, Y501, and H505 are shown in sticks. The RBD of Omicron and ACE2 are shown in blue and salmon, respectively.

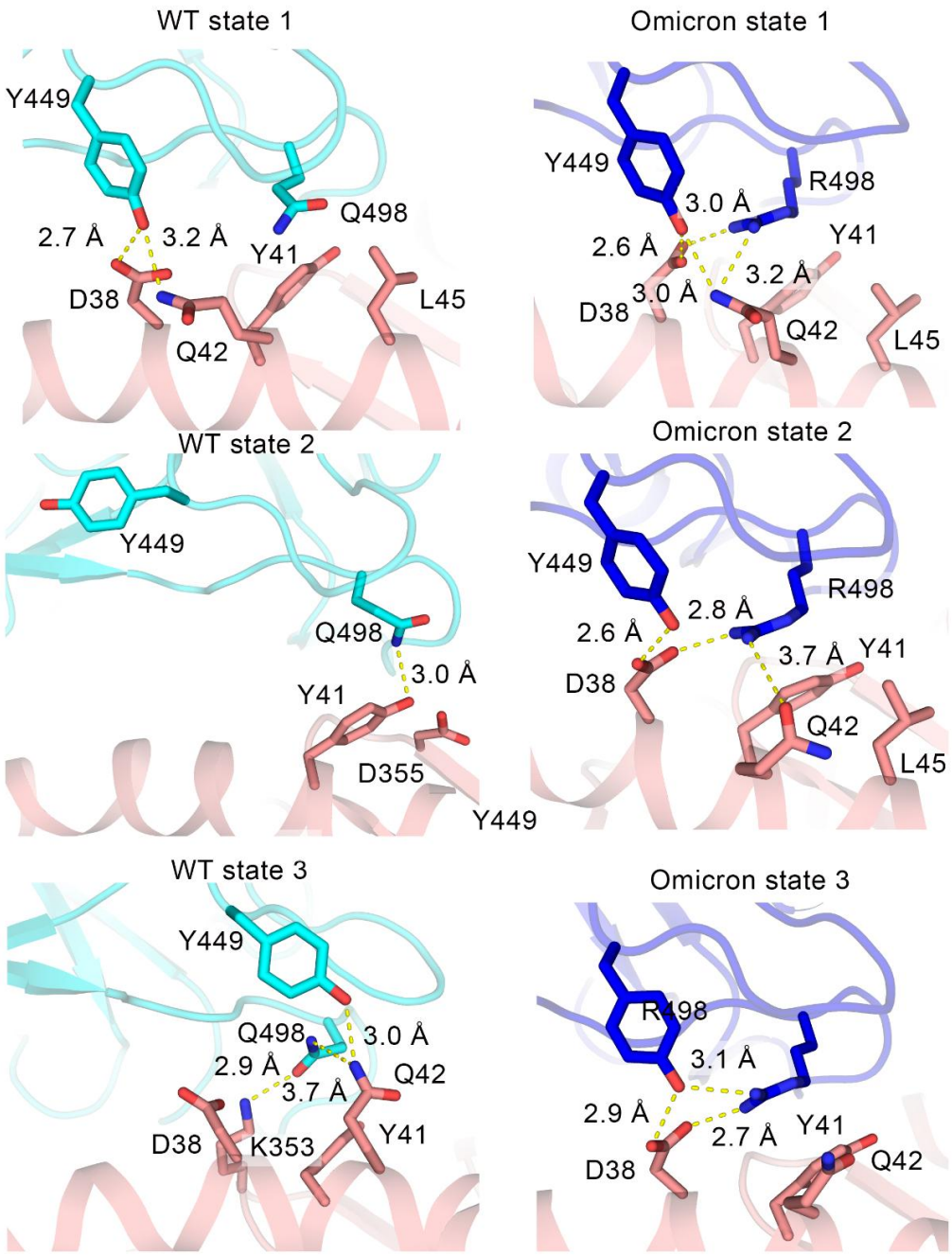

Extended Data Fig. 3 The interactions between Y449 and Q/R498 of RBD with ACE2 in WT and Omicron systems. The residues in ACE2 within 5 Å to Y449 and Q/R498 are shown in sticks while interactions are shown in yellow dashed lines. The RBD of WT, the RBD of Omicron and ACE2 are shown in cyan, blue and salmon, respectively. In WT system, Y449 shows a unique horizontal pose in state 2 which is unseen in other states. The loss of interactions with D38 and Q42 may lead to the decrease of Y449 contribution in WT state 2. In the Omicron system, however, the hydrogen bond network among D38, Q42 Y449 and R498 reduces the possibility of the horizontal conformation of Y449 and also promotes the interactions between R498 and ACE2. In WT state 3, Q498 interacts with Q42, which similarly promotes its binding affinity ($\Delta G = -5.43 \pm 2.35$ kcal/mol).

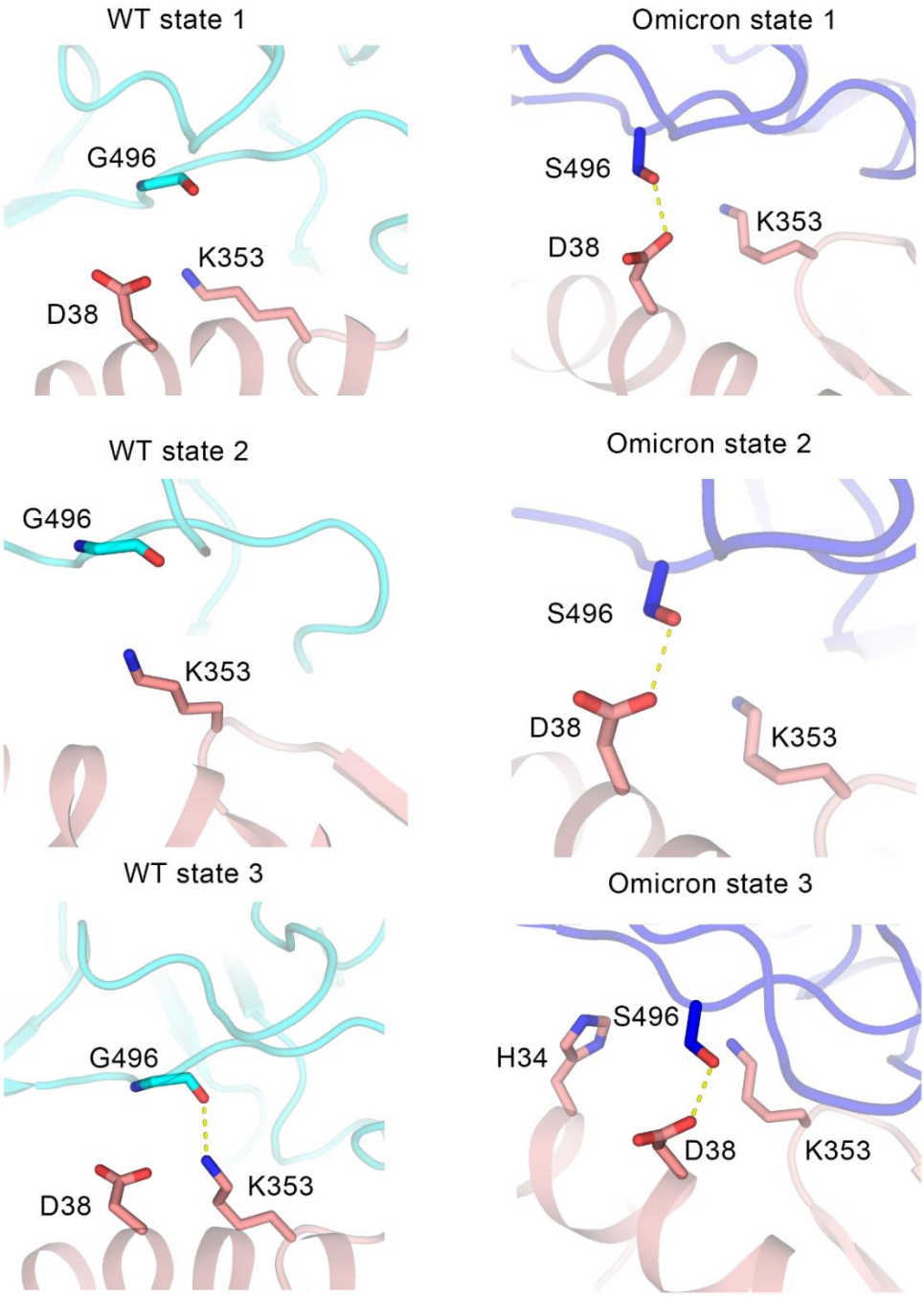

Extended Data Fig. 4 The interactions between G/S496 of RBD with ACE2 in WT and Omicron systems. The residues in ACE2 within 5 Å to G/S496 are shown in sticks while interactions are shown in yellow dashed lines. The RBD of WT, the RBD of Omicron and ACE2 are shown in cyan, blue and salmon, respectively. In WT system, G496 in state 1 and state 2 show no interaction with ACE2, leading to weak contribution to the binding affinity (-0.95 ± 1.18 and -0.01 ± 0.11 kcal/mol, respectively). As for state 3, G496 interacts with K353 in its main chain, which leads to an increase of the binding ability (-2.05 ± 1.11 kcal/mol). As a contrast, in Omicron system, S496 has interaction with D38 in all three macrostates and behaves a lower

binding free energy.

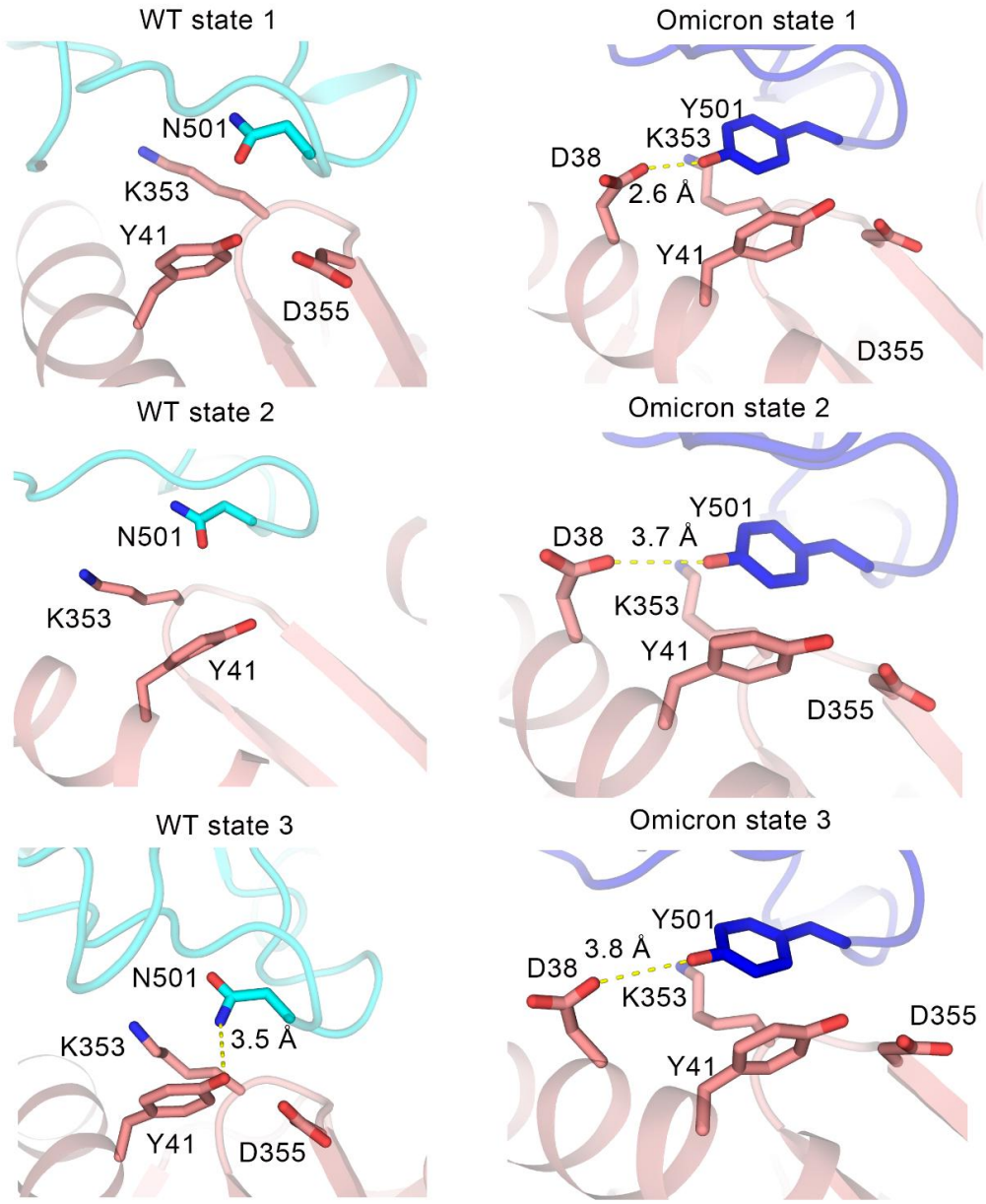

Extended Data Fig. 5 The interactions between N/Y501 of RBD with ACE2 in WT and Omicron systems. The residues in ACE2 within 5 Å to N/Y501 are shown in sticks while interactions are shown in yellow dashed lines. The RBD of WT, the RBD of Omicron and ACE2 are shown in cyan, blue and salmon, respectively. In WT system, N501 also has no interaction with ACE2 in states 1 and 2 and shows weak energy contribution (-1.14 ± 0.79 and -0.74 ± 0.77 kcal/mol, respectively). Even in WT state 3, the energy does not decrease too much with the hydrogen bond to Y41 (-2.61 ± 1.28 kcal/mol). This phenomenon may be caused by the hydrophilic sidechain of N501 embedded in a hydrophobic environment made by the sidechains of K353 and Y51. As N501Y changes to a residue with a longer sidechain and a hydrophobic phenyl ring in Omicron system, the interaction with D38 is stable in each macrostate

and the ring of tyrosine is suitable in the hydrophobic environment.